Atmos. Chem. Phys. Discuss., 15, 28361–28393, 2015
www.atmos-chem-phys-discuss.net/15/28361/2015/
doi:10.5194/acpd-15-28361-2015

Atmospheric Chemistry and Physics Discussions
Open Access

This discussion paper is/has been under review for the journal Atmospheric Chemistry and Physics (ACP). Please refer to the corresponding final paper in ACP if available.

Using proxies to explore ensemble uncertainty in climate impact studies: the example of air pollution

V. E. P. Lemaire[1], A. Colette[1], and L. Menut[2]

[1]Institut National de l'Environnement Industriel et des Risques (INERIS), Verneuil en Halatte, France
[2]Laboratoire de Météorologie Dynamique, UMR CNRS8539, Ecole Polytechnique, Ecole Normale Supérieure, Université P.M. Curie, Ecole Nationale des Ponts et Chaussées, Palaiseau, France

Received: 29 July 2015 – Accepted: 6 October 2015 – Published: 21 October 2015

Correspondence to: V. E. P. Lemaire (vincent.lemaire-etudiant@ineris.fr)

Published by Copernicus Publications on behalf of the European Geosciences Union.

Abstract

Because of its sensitivity to unfavorable weather patterns, air pollution is sensitive to climate change so that, in the future, a climate penalty could jeopardize the expected efficiency of air pollution mitigation measures. A common method to assess the impact of climate on air quality consists in implementing chemistry-transport models forced by climate projection. However, the computing cost of such method requires optimizing ensemble exploration techniques.

By using a training dataset of deterministic projection of climate and air quality over Europe, we identified the main meteorological drivers of air quality for 8 regions in Europe and developed simple statistical models that could be used to predict air pollutant concentrations. The evolution of the key climate variables driving either particulate or gaseous pollution allows concluding on the robustness of the climate impact on air quality.

The climate benefit for $PM_{2.5}$ was confirmed −0.96 (±0.18), −1.00 (±0.37), −1.16 ± (0.23) $\mu g\,m^{-3}$, for resp. Eastern Europe, Mid Europe and Northern Italy and for the Eastern Europe, France, Iberian Peninsula, Mid Europe and Northern Italy regions a climate penalty on ozone was identified 10.11 (±3.22), 8.23 (±2.06), 9.23 (±1.13), 6.41 (±2.14), 7.43 (±2.02) $\mu g\,m^{-3}$. This technique also allows selecting a subset of relevant regional climate model members that should be used in priority for future deterministic projections.

1 Introduction

The main drivers of air pollution are (i) emission of primary pollutants and precursors of secondary pollutants, (ii) long-range transport, (iii) atmospheric chemistry and (iv) meteorology (Jacob and Winner, 2009). We can thus anticipate that air quality is sensitive to climate change taking as example the link between heat waves and large scale ozone episodes (Vautard et al., 2005) as well as background changes. But in addition

ACPD
15, 28361–28393, 2015

to the direct impact of climate change on air pollution through the change in frequency and severity of synoptic conditions conducive to the accumulation of air pollutants we must also note that climate can have an impact on anthropogenic and biogenic emission of pollutants and precursors (Langner et al., 2012b) as well as on changes in the global background of pollution, and therefore long range transport (Young et al., 2013). There is therefore a concern that in the future, climate change could jeopardize the expected efficiency of pollution mitigation measures based on emission reductions. Hence the need to characterize and quantify uncertainties related to the impact of climate change.

The most widespread technique used to assess the impact of climate change on air quality consists in implementing regional climate projections in Chemistry Transport Models (CTM) (Jacob and Winner, 2009). The computational cost of such initiative is substantial given that it involves multi-annual global climate simulations, dynamical downscaling through regional climate simulations and ultimately CTM simulations. Besides the computational cost, it also raises technical difficulties in collecting, transferring and managing large amount of model data. Altogether, these difficulties led to the use of a single source of climate projections (Meleux et al., 2007; Katragkou et al., 2011; Jiménez-Guerrero et al., 2012; Langner et al., 2012b; Colette et al., 2013; Hedegaard et al., 2013; Varotsos et al., 2013) or two at most in published studies (Huszar et al., 2011; Juda-Rezler et al., 2012; Langner et al., 2012a; Manders et al., 2012; Colette et al., 2015). And the choice of such a source was often a matter of opportunity rather than an informed choice. These studies capture trends and variability but their representation of uncertainty is not satisfactory in the climate context. Moreover the divergence in climate impact between two studies for the same pollutant supports again the need of such ensemble approaches (e.g. Lecœur et al., 2014 find a climate benefit for $PM_{2.5}$ in Europe while Manders et al., 2012, suggest the opposite). Thus the lack of multi-model approach in air quality and climate projections is a serious caveat that needs to be tackled in order to comply with best practices in the field of climate impact research, where ensemble approaches is state of the art.

ACPD
15, 28361–28393, 2015

Hence, in order to assess the climate uncertainties on surface ozone and particulate matter over Europe in a changing climate, we developed a new method which avoids forcing a CTM with an ensemble of climate models. It consists in using a simple statistical model applied to an ensemble of regional climate projections.

Using a training dataset of deterministic projection of climate and air quality over Europe, we identified the main meteorological drivers of air quality for 8 regions in Europe and developed corresponding simple statistical models that could be used to predict air pollutant concentrations. These statistical models are subsequently applied to an ensemble of regional climate models (Jacob et al., 2014) to assess the robustness of the air quality projections. By discussing the evolution of the key climate variables of each member of the climate ensemble driving either particulate or gaseous pollution we can conclude on the robustness of the climate impact on air quality. Besides allowing a quantification of uncertainties, this technique also allows selecting a subset of relevant regional climate model members that should be used in priority for future ensemble deterministic projections.

The use of such a methodology is inspired from earlier work in the field of hydrology, where Vano and Lettenmaier (2014) have estimate future stream-flow by using a sensitivity-based approach which could be applied to generate ensemble simulations. Such hybrid statistical and deterministic approach have also been used in the past in the field of air quality, but mostly for near-term forecasting, relying on statistical models of various complexity (i.e. Land Use Regression, Neural Network, Nonlinear regression, Generalized Additive Models...) (Prybutok et al., 2000; Schlink et al., 2006; Slini et al., 2006). The most relevant example in the context of future air quality projection is that of (Lecœur et al., 2014), that use the technique of wind regime analogues, although they did not apply their approach to an ensemble of climate projection.

This paper deals with all the steps needed to build the proxy of ensemble and the results obtained. First (Sect. 2) we present the methods and input data: the design of the statistical model of the air quality response to meteorological drivers is presented as well as the deterministic modelling framework used to create our training dataset.

ACPD
15, 28361–28393, 2015

Section 3 focuses on results. The deterministic air quality projections are presented for ozone peaks and $PM_{2.5}$ in Sect. 3.1. The selected statistical models for each region are evaluated in Sect. 3.2. The relevance of the statistical method to evaluate uncertainties and optimize ensemble exploration is discussed in Sect. 4.

2 Development of statistical models of the air quality response to meteorological variability

2.1 Method

We consider ozone and $PM_{2.5}$ as the main pollutants of interest for both purposes: public health (Dockery and Pope, 1994; Jerrett et al., 2009) and climate interactions (IPCC 2013). For both of them, simple linear models have been developed using meteorological variables as predictants: near surface temperature (T2m), daily precipitation, incoming short wave radiation, planetary boundary layer (PBL) depth, surface wind (U10m) and specific humidity.

The choice of these meteorological variables is based on an analysis of the literature on phenomenological links between air pollution and meteorology. For $PM_{2.5}$, turbulent mixing, often related to the depth of the planetary boundary layer, dominates (McGrath-Spangler et al., 2015). Decrease of PBL depth is both related to (i) the concentration of pollutants (Jiménez-Guerrero et al., 2012) and (ii) their dry deposition because of the vicinity of surface receptors (Bessagnet et al., 2010). The wind plays also multiple roles. High wind speed favors the dilution of particulate matter (Jacob and Winner, 2009) but enhances sea-salt and dust mobilization (Lecœur and Seigneur, 2013). Precipitation is often reported as a major sink of $PM_{2.5}$ through wet scavenging (Jacob and Winner, 2009). Water vapor, through specific humidity, participates in aerosol formation during nucleation processes. Moreover it can have an impact on the rates of certain chemistry reactions, as well as temperature. The temperature impacts are difficult to isolate because of the $PM_{2.5}$ mix of components (organic, inorganic, dust,

ACPD
15, 28361–28393, 2015

sea-salt...) and compensating effects. For instance, according to (Jacob and Winner, 2009), a temperature rise has opposite effects for sulfate and nitrate (resp. increase and decrease concentrations). But for the overall $PM_{2.5}$ mass, an increase in temperature will decrease the concentration as a result of higher volatility and subsequent higher aerosol to gas phase conversion (Megaritis et al., 2014). In the case of the chemistry and transport model used in this study, CHIMERE (Menut et al., 2013), the volatile species in the gas and aerosol phases are assumed to be in chemical equilibrium. This thermodynamic equilibrium, computed by ISORROPIA (Fountoukis and Nenes, 2007), is driven by temperature and humidity and conditions the concentration of several aerosol species (ammonium, sodium, sulfate, nitrate and so on). Thus a major role of these variables is expected in this study.

The impact on ozone or its precursors are presented here. A temperature rise catalyzes atmospheric chemistry (Doherty et al., 2013). Moreover increasing temperature and solar radiation enhance isoprene emission which is a biogenic precursor of ozone (Langner et al., 2012b; Colette et al., 2013). Finally changing the amount of incoming short wave radiation will play a role on the photochemistry. Indeed short wave radiation contributes both as a sink (water vapor and radiation leads to ozone photolysis) and a source (nitrogen dioxide photolysis produces ozone) of ozone (Doherty et al., 2013). The PBL effect on ozone varies with the meteorological conditions. Increasing the depth dilutes the ozone concentrations, but it also favors the mixing of its precursors which leads to an ozone concentrations increase (Jacob and Winner, 2009). The amount of water vapor in the atmosphere mostly drives the abundance of the hydroxyl radical (OH). OH is implied in ozone destruction through several processes (i.e. photolysis, HNO_3 production) (Varotsos et al., 2013). It is also implied in ozone production via the formation of NO_2. Some VOC are oxidized by OH and form RO_2 which reacts with NO to form NO_2, a precursor of ozone (Seinfeld and Pandis, 2008).

The design of the statistical model is deliberately limited to a simple bivariate linear least square based using two meteorological variables. In order to facilitate the geophysical interpretation, using meteorological variables instead of a linear combination

ACPD
15, 28361–28393, 2015

of multiple variables (i.e. Prior Principal Component Analysis axes) is preferred. The main caveat is that it implies independence between meteorological variables.

While the skill of the statistical model could have improved by using a prior principal component analysis, a non-linear model, or more than 2 predictors, we considered that remaining in a 2-D physical parameter space was important for the purpose of the discussion as will be illustrated below. Hence the accuracy of the statistical proxy could be refined but we argue that our approach is satisfactory to assess uncertainty and optimize ensemble exploration.

Such a statistical model is built for each of the eight European climatic regions set in the PRUDENCE project (Christensen and Christensen, 2007). These regions are: British Isles (BI), Iberian Peninsula (IP), France (FR), Mid Europe (ME), Scandinavia (SC), Northen Italy (NI – referred to as the Alps in Climate studies but chiefly influenced by the polluted Po-Valley in the air quality context), Mediterranean (MD) and Eastern Europe (EA). For each of these regions, a spatial average of predictants (meteorological variables) and predicted (concentrations) values is taken. The statistical model is based on daily averages for all meteorological and air pollutant concentrations except ozone for which the daily maximum of 8 h running means is used. The seasonality is removed by subtracting the average seasonal cycle over the historical period.

2.2 Training and validation datasets

The datasets used to fit and test the statistical models are produced by the regional climate and air quality modelling framework presented in Colette et al. (2013). By using a full suite of models covering both climate and chemistry from the global to the regional scale, they could produce long term air quality projections over Europe. The Earth System Model (ESM) which drives these simulations is the IPSL-CM5A-MR (Dufresne et al., 2013). The global data used in this study were produced for the Coupled Model Intercomparison Project Phase 5 initiative (CMIP5) (Taylor et al., 2012; Young et al., 2013). Then the climate data obtained by the ESM are dynamically downscaled by the regional climate model WRF (Skamarock et al., 2008). The spatial resolution is 0.44°

ACPD
15, 28361–28393, 2015

Uncertainty in climate impacts on air quality

V. E. P. Lemaire et al.

over Europe (Colette et al., 2013). These simulations were part of the low-resolution simulations performed within the framework of the European-Coordinated Regional Climate Downscaling Experiment program (EURO-CORDEX) (Jacob et al., 2014). The corresponding hindcasts were evaluated in Kotlarski et al. (2014). Finally the regional climate fields are used to drive the CTM CHIMERE (Menut et al., 2013), for the projection of air quality under changing climate. Since we are only interested in the effect of climate change, pollutant emissions remain constant at their level of 2010, as prescribed in the ECLIPSE-V4a dataset (Klimont et al., 2015). Similarly, chemical boundary conditions prescribed with the INCA model (Hauglustaine et al., 2014) as well as the land-use are also kept constant.

The training dataset used to build the statistical models is the historical air quality simulations (1976–2005), while future air quality and climate projections will be used for testing purposes. In order to evaluate the uncertainty related to climate change, the statistical models should be efficient to reproduce the pollutant concentrations over the historical period (training period) and to predict them (testing period). We choose the future time period as validation dataset in order to challenge the statistical model trained over a given validity range that is expected to be exceeded in the future. The different tests performed are explained Sect. 3.2.

2.3 Regional climate projection ensemble

To evaluate the uncertainty, the statistical model of air quality is used in predictive mode using the regional climate projections performed in the framework of the EURO-CORDEX program (Jacob et al., 2014). The combinations of global/regional climate models used here are: CanESM2/RCA4; CSIRO-Mk3-6-0/RCA4; CNRM-CM5-LR/RCA4; EC-EARTH/RACMO2; EC-EARTH/RC4; GFDL-ESM2M/RCA4; IPSL-CM5A-MR/RCA4; IPSL-CM5A-MR/WRF; MIROC5/RCA4; MPI-ESM-LR/RCA4; MPI-ESM-LR/CCLM; NorESM1-M/RCA4 (see Jacob et al., 2014, for details on the model nomenclature).

ACPD
15, 28361–28393, 2015

The performances of the global models used to drive the regional projections have been evaluated (Jury, 2012; Cattiaux et al., 2013). The performances of the regional model driven by the ERA-Interim have been explored in Kotlarski et al. (2014). No study has evaluated the bias of the global/regional combinations even if it could be relevant since the combination of a driving model and a regional model is not the simple addition of their bias. It is therefore safer to use such data to assess relative changes rather than absolute levels.

3 Results

In this part we studied the end (2071–2100) of the century, for one scenario (RCP8.5). This 30 years period is chosen to be representative regardless of the inter-annual variability (Langner et al., 2012a). The RCP8.5 is a highly energy-intensive scenario (radiative forcing level equal to $8.5\,\mathrm{W\,m^{-2}}$) (van Vuuren et al., 2011). We focus on the RCP8.5 and the end of the century to obtain the most significant results.

3.1 Climate and air quality projections

3.1.1 $PM_{2.5}$

Figure 1a represents the 30 years average $PM_{2.5}$ concentrations over the historical period (1976 to 2005). Higher concentrations are modeled over European pollution hotspots: Benelux, Po Valley, Eastern Europe and large cities. A similar pattern is found in the future (RCP8.5 – average over the period 2071–2100) albeit with lower concentrations (Fig. 1b). The difference (future minus historical) is given in Fig. 1c where the statistical significance of the changes was represented by black points at each grid points and evaluated by a Student *t* test with Welch variant at the 95 % confidence level based on annual mean. The decrease is statistically significant over most of the domain.

ACPD
15, 28361–28393, 2015

Title Page
Abstract Introduction
Conclusions References
Tables Figures
◀◀ ▶▶
◀ ▶
Back Close
Full Screen / Esc
Printer-friendly Version
Interactive Discussion

Overall, we identify a climate benefit on particulate matter pollution similarly to Colette et al. (2013), Lecœur et al. (2014) but in opposition to Manders et al. (2012). Hedegaard et al. (2013) finds a decrease in high latitude and an increase in low latitude. The role of future precipitation projections and more efficient wet scavenging has often been pointed out to explain such a future evolution of particulate matter (Jacob and Winner, 2009). However, the lack of robustness in precipitation evolution over major European particulate pollution hotspots in regional climate models (Jacob et al., 2014) challenges the confidence we can have in single model air quality and climate projection, supporting again the need for ensemble approaches.

3.1.2 Ozone peaks

Figure 1d represents the summer (JJA) average ozone daily maximum concentrations over the historical period (1976–2005). A North–South gradient appears with lower concentration in the North and higher concentration fields over the Mediterranean Sea. The Fig. 1e corresponds to the summer average ozone projection of the RCP8.5 at the end of the century (2071–2100). A similar pattern is found, with higher concentrations in the southern part of the domain. The map of the difference, Fig. 1f, (RCP8.5 – actual) indicates an increase of ozone concentrations over Eastern Europe, Mediterranean land surfaces, and North Africa and a decrease over British Isles and Scandinavia. Most of the changes are statistically significant except over West Europe. This concentration rise is frequently associated to an increase of temperature in the literature (Meleux et al., 2007; Katragkou et al., 2011), see Sect. 2 above for an review of physical and chemical processes underlying this association.

Following Langner et al. (2012b), Manders et al. (2012) and Colette et al. (2013, 2015) we confirm overall the fact that climate change constitutes a penalty for surface ozone in Europe.

ACPD
15, 28361–28393, 2015
Uncertainty in climate impacts on air quality
V. E. P. Lemaire et al.

3.2 Statistical models

Here we introduce the statistical models trained over the historical period. First we discuss the expected impact of key meteorological processes on pollutants concentration on the basis of the model correlation and put our results in perspective with the key driving factors reported in the literature. Then we evaluate the performance of statistical models over the future period in order to discard regions and pollutants where the skill of the statistical model is too small to draw robust conclusions on the uncertainties of projections.

3.2.1 $PM_{2.5}$

The skill and predictors for bivariate linear least square statistical models fitted for each region are given in Table 1. The depth of the planetary boundary layer is identify as the major meteorological driver for $PM_{2.5}$ which is a different finding compared to (Megaritis et al., 2014) who report a smaller impact for the PBL depth. Near surface temperature is often selected as second predictor. The wind is pointed out as a relevant predictor twice and only for coastal regions (resp. BI and MD) where the sea-salt dominates. Last, precipitation is selected only once as 2nd variable for the Iberian Peninsula (IP). It could be partly due to our choice of a linear correlation whereas a logical regression would have been more efficient given that PM correlations are sensitive to the presence/absence of precipitation rather than their intensity. It is difficult to assess objectively whether the larger role of temperature than precipitation in our findings is an artifact related to the design of the statistical model. The importance of precipitation in the impact of climate change on particulate pollution is often speculated in the literature, with little quantitative evidence. The bilinear model used here is simplistic, but it offers an objective quantification of that role. It should be added that the importance of temperature is well supported by the volatilization process for SIA and SOA. It is also supported by the pattern of projected $PM_{2.5}$ change, which is spatially correlated with present-day $PM_{2.5}$ concentration. This spatial correlation suggests an impact of a uniform driver which points towards temperature rather than precipitation change that exhibits a strong north–south gradient in Europe.

Then the predictive skill of these models is tested over the period 2071–2100 by computing the Normalized Root Mean Squared Error (NRMSE) between the statistically predicted $PM_{2.5}$ (concentrations estimated with the statistical models), and the results of the deterministic regional air quality and climate modelling suite presented in Sect. 2.2.

Figure 2 shows, for each region, the scatter between r-squared over the historical period and the NRMSE in predictive mode for the RCP8.5 at the end of the century. The NRMSE is equal to the RMSE divided by the standard deviation of the reference: air quality projection (2071–2100). It allows describing the predictive power of a model, if the result is "less or equal to 1" then the model is a better predictor of the data than the data mean (Thunis et al., 2012). We expect regions where the correlation over the historical period is low to be poorly captured by the statistical model in the future. The fact that the good correlation for EA and ME are associated with a NRMSE around 0.7 in the future indicates either that the main meteorological drivers in the future will remain within their range of validity or that extrapolation is a viable approximation.

This feature gives confidence in using statistical models for these regions in predictive mode. For the NI region, the NRMSE is acceptable (below 0.85) even if the r-squared is low.

Considering that the model skill was satisfactory for the EA, ME and NI regions, we decided to focus on these regions for the uncertainty assessment in the remainder of this paper.

3.2.2 Ozone peaks

For summertime ozone peaks, as expected, near surface temperature and incoming short wave radiation are identified as the two main meteorological drivers for most regions (cf. Table 2). Concerning the region EA, the drivers are near surface temperature and specific humidity. The skill of the statistical model is very low over the British Isles

ACPD
15, 28361–28393, 2015

and Scandinavia. This is because ozone pollution in these regions is largely influenced by the long range transport of air pollution. It is therefore poorly correlated with the local variability of meteorological variables. The poor performances of the statistical model over the Mediterranean region are more surprising. The lower variability of temperature and incoming shortwave radiation in this region makes them less relevant to explain ozone concentrations.

The linear models that are ultimately considered efficient enough in terms of correlation to capture the ozone concentrations over the historical period are those of the following regions: EA, FR, IP, ME and NI.

This selection is further supported by applying the same approach as for $PM_{2.5}$ to evaluate the predictive skill of the models. The regions mentioned above where the correlation of the statistical model is low (BI, SC and MD) stand out on this graph (cf. Fig. 2). So that the regions: EA, FR, IP, ME and NI are selected for the uncertainty assessment in the remainder of this paper.

4 Evaluation of the uncertainty

To evaluate the robustness of the air quality and climate projection we use the statistical models introduced in Sect. 2 applied to regional climate projections to develop a proxy of ensemble of air quality and climate projections for each region. This proxy of ensemble will be used to identify the subset of regional climate projections that should be used in priority in the deterministic modelling suite, but it can also given an indication on the robustness of the climate impact on air quality by comparing the evolution of key climate drivers.

4.1 $PM_{2.5}$

In order to assess qualitatively the robustness of the evolution of regional climate variables having an impact on air quality, we first design a 2-D parameter space where the isopleths of statistically predicted pollutant concentrations are displayed (background of Fig. 3). Then the distributions of historical and future meteorological variables as extracted from the regional climate projections are added to this parameter space. For each Regional Climate Projection, we show the average of the two driving meteorological variables as well as the 70th percentile of their 2-D-density plot, i.e. the truncation at the 70th quantile of their bi-histogram which means that 70 % of the simulated days lie within the contour. Both historical and future climate projections (here for the RCP8.5 scenario and the 2071–2100 period) are displayed on the parameter space. The climate projections are all centered on the IPSL-CM5A-MR/WRF member so that only the distribution of the later stands out for the historical period.

As pointed out in Table 1, the main meteorological drivers are the depth of the PBL and near surface temperature for the example of Eastern Europe region displayed on Fig. 3. The statistically modeled isopleths in the background of the figure show that $PM_{2.5}$ concentration decrease when the depth of the PBL increases (x axis), or when temperatures increase (y axis). The comparison of historical and future distributions shows that, even though the PBL depth constitutes the most important meteorological driver for $PM_{2.5}$, it does not evolve notably in the future (cf. Fig. 3). On the contrary, the secondary driver (surface temperature) increases significantly, leading to a decrease of $PM_{2.5}$ concentrations. The small spread of RCMs in terms of both evolution of PBL depth and temperature suggests that this climate benefit on particulate pollution is a robust feature. However, on Fig. 3, CSIRO-Mk3-6-0/RCA4 and MPI-ESM-LR/CCLM present respectively the largest and the smallest $PM_{2.5}$ concentrations decrease. Those isopleths present the same characteristics for ME and NI regions (cf. Figs. S1 and S4 in the Supplement).

The qualitative evolution represented on Fig. 3 is further quantified by applying the linear model to the future meteorological variables in the regional climate projections. These results are represented by the probability density functions of the predicted concentrations of each GCM/RCM couple minus the estimated values for the historical run (e.g. 2071–2100 vs. 1976–2005; cf. Fig. 4). For EA and ME, the longer tail of the probability density function of MPI-ESM-LR/CCLM compare to the average of the models reflects that stronger pollution episode will occur in the future even if the mean of the concentrations are lower than the average of the ensemble (cf. Fig. 4 for EA and Fig. S2 for ME).

Besides the distribution, the ensemble mean and standard deviation of the estimated projected change in $PM_{2.5}$ concentrations has been quantified (Table 3). All the selected regions depict a significant decrease of the $PM_{2.5}$ concentrations across the multi-model proxy ensemble indicating that the climate benefit on particulate matter in a robust feature in these regions. The magnitude of the decrease depends on the region and is expressed as follow ensemble mean (± standard deviation): −0.96 (±0.18), −1.00 (±0.37), −1.16 (±0.23) $\mu g\,m^{-3}$, for resp. EA, ME and NI (cf. Table 3).

In order to explain the differences in the response of individual RCM in the ensemble, we need to explore the historical meteorological variables PDF and to compare them with the evolution of IPSL-CM5A-MR/WRF. The comparison of the historical distribution for the temperature reflects the stronger extremes of IPSL-CM5A-MR/WRF (e.g. colder than the others when it is cold). Only in NI our model lies in the mean of the ensemble. Concerning the PBL depth, the values are similar than the average of the ensemble for ME even if MPI-ESM-LR/RCA4 and EC-EARTH/RACMO2 present the largest values. IPSL-CM5A-MR/WRF has a thinner boundary layer for NI and a larger for EA than the average but the differences are limited (cf. Fig. 5).

CSIRO-Mk3-6-0/RCA4 depicts the most important decrease for all the selected regions except over NI where it is exceed by CanESM2/RCA4 (resp. 1.51 vs. 1.61 $\mu g\,m^{-3}$; cf. Table 3). This is linked to a larger temperature rise compare to the other models and a larger boundary layer height evolution compare to the other member of the ensemble for these regions (cf. Fig. 3). CanESM2/RCA4 and CSIRO-Mk3-6-0/RCA4 reflects the same finding for the region ME.

MPI-ESM-LR/CCLM presents the smallest decrease of $PM_{2.5}$ for each of the selected regions (e.g. over ME is almost 3 times smaller than the largest decrease). As already mentioned above, the particular tails of the distributions for EA and ME indicate more pollution episodes in the future. The historical distributions exhibit a larger boundary layer than the average models of the ensemble and a similar temperature. Thus, the low $PM_{2.5}$ concentration decrease is explained by the small evolution of the meteorological drivers as shown by the Fig. 3. The evolution of the PBL depth depicts the relevance of this meteorological variable: a large part of the contour overlaps the red part of the background. Hence it indicates more days with a thinner layer which is directly related to more PM_{25} pollution episodes.

Overall we conclude that the climate benefit is confirmed for the $PM_{2.5}$ for each selected regions. The result is robust since all the proxy of ensemble built with the bivariate statistical model applied to regional climate projection present similar density functions and average projected changes. The regional climate models that exhibit a specific response are CanESM2/RCA4; CSIRO-Mk3-6-0/RCA4 and MPI-ESM-LR/CCLM, which should therefore be considered for a more in-depth evaluation using explicit deterministic projections.

4.2 Ozone peaks

For most of the selected regions (FR, IP, ME and NI,) the main drivers are the same (i.e. near surface temperature and short wave radiation) except for EA where the major drivers are temperature and specific humidity. As discussed above for $PM_{2.5}$, every figure (Figs. 3, S1, and S4) shows an offset of the 2-D-density plot along the temperatures axe. The projected future is warmer than the historical period. According to the ozone concentrations predicted by the linear model (displayed in the background of Fig. 3) these offsets lead to more ozone episodes. This trend appears for the entire models ensemble so that we can conclude with confidence that this climate penalty is a robust feature even if the specific distribution shape of some of the models stand out (CanESM2/RCA4; CNRM-CM5-LR/RCA4; CSIRO-Mk3-6-0/RCA4; IPSL-CM5A-MR/WRF).

The ozone increase of the ensemble is equal 10.11 (±3.22), 8.23 (±2.06), 9.23 (±1.13), 6.41 (±2.14), 7.43 (± 2.02) $\mu g\,m^{-3}$ for EA, FR, IP, ME and NI (cf. Table 3).

ACPD
15, 28361–28393, 2015
Uncertainty in climate impacts on air quality
V. E. P. Lemaire et al.

Title Page
Abstract Introduction
Conclusions References
Tables Figures
◄ ►
Back Close
Full Screen / Esc
Printer-friendly Version
Interactive Discussion

These values confirm the statistically significant climate penalty (the mean is at least two times larger than the standard deviation). However, as already mentioned for Fig. 3, we find differences among the models. Here the meteorological variables and their evolution are discussed to explain these differences. The meteorological distributions are slightly different between the models of the ensemble: the summertime temperature predicted by IPSL-CM5A-MR/WRF has stronger extremes than the other models. Moreover it is warmer than the ensemble in EA. The specific humidity is around 1.5 times larger for IPSL-CM5A-MR/WRF than for the other models. Concerning the last meteorological variable, incoming short wave radiation, IPSL-CM5A-MR/WRF lies in the average (cf. Figs. S6 and S9). Only EC-EARTH/RACMO2 and MPI-ESM-LR/RCA4 exhibits lower values (around half of the average for MPI-ESM-LR/CCLM).

The magnitude of the ozone rise changes between the models and the regions. Note that CanESM2/RCA4 exhibits the most important discrepancy (i.e. around 1.5 times the ensemble mean) followed by CSIRO-Mk3-6-0/RCA4 for each selected regions. This is explained by the significant temperature increase during summertime which is the major driver, as identified by the statistical models, of ozone concentration. Note that the value is skyrocketing for the region EA when specific humidity is the 2nd predictor, 4 times the value of IPSL-CM5A-MR/WRF, the lower increase. CNRM-CM5-LR/RCA4 presents the 2nd lowest increase.

On the contrary the lower increase of the summer temperature and sometimes a decrease of the incoming short wave radiation amount (e.g. IPSL-CM5A-MR/WRF in NI) are associated to lower ozone concentration changes for IPSL-CM5A-MR/WRF and CNRM-CM5-LR/RCA4 for FR, IP, ME and NI (cf. Table 3).

On the Fig. S5, we can point out the particular pattern of the MPI-ESM-LR/CCLM distribution for the NI region: a wide and flat Gaussian with large tails. The ozone rise would be more pronounced for the upper quantile which depicts more extreme polluted episode.

Overall the climate penalty is confirmed even if some regional climate models stand out of the distribution, such as CanESM2/RCA4; CNRM-CM5-LR/RCA4 and CSIRO-

ACPD
15, 28361–28393, 2015

Mk3-6-0/RCA4 which should therefore be considered for further deterministic projections.

5 Conclusions

An alternative technique to assess the robustness of projections of the impact of climate change on air quality has been introduced. Using a training dataset consisting of long-term deterministic regional climate and air quality projections, we could build simple statistical models of the response of ozone and particulate pollution to the main climate drivers for several regions of Europe. Applying such statistical models to an ensemble of regional climate projection leads to the development of an ensemble of proxy projections of air quality under various future climate forcing. The assessment of the spread of the ensemble of proxy projections allows inferring the robustness of the impact of climate change, as well as selecting a subset of climate models to be used in priority for future explicit air quality projections, therefore proposing a smart exploration of the ensemble.

The main climate drivers that were identified are (i) for $PM_{2.5}$: the boundary layer depth and the near surface temperature and (ii) for ozone: the near surface temperature and the incoming short wave radiation except for Eastern Europe where specific humidity is the second predictor. The skill of the statistical models depends on the regions of Europe and the pollutant.

For $PM_{2.5}$ and the regions Eastern Europe (EA) and Mid Europe (ME), a bivariate linear least square captures about 50 % of the variance. But for British Isles (BI) and Scandinavia (SC), where air pollution is largely driven by long range transport, such a simple and local approach is not able to reproduce the variability of pollutant concentrations.

The ozone concentrations are well reproduced by the statistical model for the following regions: Eastern Europe (EA), France (FR), Iberian Peninsula (IP), Mid Europe (ME) and Northen Italy (NI). The meteorological variables are not discriminating

ACPD
15, 28361–28393, 2015

enough to depict the pollutant concentration for Mediterranean region. For the regions where the performances of the statistical model were considered satisfactory, a proxy of the future pollutant concentrations could be estimated (i.e. (i) EA, ME and NI, (ii) EA, FR, IP, ME and NI).

An overall climate benefit for $PM_{2.5}$ was found in the proxy ensemble of climate and air quality projections. The ensemble mean change is −0.96 (standard deviation: ±0.18), −1.00 (±0.37), −1.16 (±0.23) $\mu g\,m^{-3}$, for resp. EA, ME and NI. This beneficial impact of climate change for particulate matter pollution is in agreement with the deterministic projections of Huszar et al. (2011), Juda-Rezler et al. (2012), Colette et al. (2013) but in opposition to Manders et al. (2012). These differences could be partly explained by the different time windows (i.e. 2060–2041 vs. 2100–2071), climate scenario (i.e. A1B which is similar to RCP6.0 vs. RCP8.5) and pollutant (i.e. PM_{10} vs. $PM_{2.5}$).

For all the selected regions a robust climate penalty on ozone was identified: 10.11 (±3.22), 8.23 (±2.06), 9.23 (±1.13), 6.41 (± 2.14), 7.43 (±2.02) $\mu g\,m^{-3}$ for resp. EA, FR, IP, ME and NI. This finding is in line with previous studies (Meleux et al., 2007; Huszar et al., 2011; Katragkou et al., 2011; Jiménez-Guerrero et al., 2012; Juda-Rezler et al., 2012; Langner et al., 2012a, b; Colette et al., 2013, 2015; Hedegaard et al., 2013; Varotsos et al., 2013).

The robustness of the impact of climate change on air quality inferred from this proxy of ensemble cannot be considered as a very definitive statement given that the underlying statistical model does not capture all the variance of the air quality response to climate change. The somewhat simple structure of the statistical model and the use of a single set of deterministic projection for its training/validation, are additional limitations of the approach. However, besides this information on the robustness, this proxy approach also allows pointing out regional climate models that should be investigated in priority in the context of deterministic model projection, therefore proposing a smart exploration of the ensemble of projections.

ACPD
15, 28361–28393, 2015

Finally, this method, applied here for air quality projection opens also the way for such approaches in other climate impact studies, where quantifying uncertainties using low computational demand is desirable.

The Supplement related to this article is available online at doi:10.5194/acpd-15-28361-2015-supplement.

Acknowledgement. The climate and air quality projections used in the present study were produced as part of the European Union's Seventh Framework Programme (FP7/2007-2013) under grant agreement no. 282687 (ATOPICA) and computing resources of the TGCC/CCRT/CEA.

References

Bessagnet, B., Seigneur, C., and Menut, L.: Impact of dry deposition of semi-volatile organic compounds on secondary organic aerosols, Atmos. Environ., 44, 1781–1787, doi:10.1016/j.atmosenv.2010.01.027, 2010.

Cattiaux, J., Douville, H., and Peings, Y.: European temperatures in CMIP5: origins of present-day biases and future uncertainties, Clim. Dynam., 41, 2889–2907, doi:10.1007/s00382-013-1731-y, 2013.

Christensen, J. and Christensen, O.: A summary of the PRUDENCE model projections of changes in European climate by the end of this century, Climatic Change, 81, 7–30, doi:10.1007/s10584-006-9210-7, 2007.

Colette, A., Bessagnet, B., Vautard, R., Szopa, S., Rao, S., Schucht, S., Klimont, Z., Menut, L., Clain, G., Meleux, F., Curci, G., and Rouïl, L.: European atmosphere in 2050, a regional air quality and climate perspective under CMIP5 scenarios, Atmos. Chem. Phys., 13, 7451–7471, doi:10.5194/acp-13-7451-2013, 2013.

Colette, A., Andersson, C., Baklanov, A., Bessagnet, B., Brandt, J., Christensen, J. H., Doherty, R., Engardt, M., Geels, C., Giannakopoulos, C., Hedegaard, G. B., Katragkou, E., Langner, J., Lei, H., Manders, A., Melas, D., Meleux, F., Rouil, L., Sofiev, M., Soares, J., Stevenson, D. S., Tombrou-Tzella, M., Varotsos, K. V., and Young, P.: Is the ozone climate penalty robust in Europe?, Environ. Res. Lett., 10, 084015, doi:10.1088/1748-9326/10/8/084015, 2015.

Dockery, D. W. and Pope, C. A.: Acute respiratory effects of particulate air pollution, Annu. Rev. Publ. Health, 15, 107–132, doi:10.1146/annurev.pu.15.050194.000543, 1994.

Doherty, R. M., Wild, O., Shindell, D. T., Zeng, G., MacKenzie, I. A., Collins, W. J., Fiore, A. M., Stevenson, D. S., Dentener, F. J., Schultz, M. G., Hess, P., Derwent, R. G., and Keating, T. J.: Impacts of climate change on surface ozone and intercontinental ozone pollution: a multi-model study, J. Geophys. Res.-Atmos., 118, 3744–3763, doi:10.1002/jgrd.50266, 2013.

Dufresne, J. L., Foujols, M. A., Denvil, S., Caubel, A., Marti, O., Aumont, O., Balkanski, Y., Bekki, S., Bellenger, H., Benshila, R., Bony, S., Bopp, L., Braconnot, P., Brockmann, P., Cadule, P., Cheruy, F., Codron, F., Cozic, A., Cugnet, D., de Noblet, N., Duvel, J. P., Ethé, C., Fairhead, L., Fichefet, T., Flavoni, S., Friedlingstein, P., Grandpeix, J. Y., Guez, L., Guilyardi, E., Hauglustaine, D., Hourdin, F., Idelkadi, A., Ghattas, J., Joussaume, S., Kageyama, M., Krinner, G., Labetoulle, S., Lahellec, A., Lefebvre, M. P., Lefevre, F., Levy, C., Li, Z. X., Lloyd, J., Lott, F., Madec, G., Mancip, M., Marchand, M., Masson, S., Meurdesoif, Y., Mignot, J., Musat, I., Parouty, S., Polcher, J., Rio, C., Schulz, M., Swingedouw, D., Szopa, S., Talandier, C., Terray, P., Viovy, N., and Vuichard, N.: Climate change projections using the IPSL-CM5 Earth System Model: from CMIP3 to CMIP5, Clim. Dynam., 40, 2123–2165, doi:10.1007/s00382-012-1636-1, 2013.

Fountoukis, C. and Nenes, A.: ISORROPIA II: a computationally efficient thermodynamic equilibrium model for K^+ Ca^{2+} Mg^{2+} NH_4^+ Na^+ SO_4^{2-} NO_3^- Cl^- H_2O aerosols, Atmos. Chem. Phys., 7, 4639–4659, doi:10.5194/acp-7-4639-2007, 2007.

Hauglustaine, D. A., Balkanski, Y., and Schulz, M.: A global model simulation of present and future nitrate aerosols and their direct radiative forcing of climate, Atmos. Chem. Phys. Discuss., 14, 6863–6949, doi:10.5194/acpd-14-6863-2014, 2014.

Hedegaard, G. B., Christensen, J. H., and Brandt, J.: The relative importance of impacts from climate change vs. emissions change on air pollution levels in the 21st century, Atmos. Chem. Phys., 13, 3569–3585, doi:10.5194/acp-13-3569-2013, 2013.

Huszar, P., Juda-Rezler, K., Halenka, T., Chervenkov, H., Syrakov, D., Krüger, B., Zanis, P., Melas, D., Katragkou, E., Reizer, M., Trapp, W., and Belda, M.: Effects of climate change on ozone and particulate matter over Central and Eastern Europe, Clim. Res., 50, 51–68, doi:10.3354/cr01036, 2011.

ACPD
15, 28361–28393, 2015

Jacob, D., Petersen, J., Eggert, B., Alias, A., Christensen, O., Bouwer, L., Braun, A., Colette, A., Déqué, M., Georgievski, G., Georgopoulou, E., Gobiet, A., Menut, L., Nikulin, G., Haensler, A., Hempelmann, N., Jones, C., Keuler, K., Kovats, S., Kröner, N., Kotlarski, S., Kriegsmann, A., Martin, E., van Meijgaard, E., Moseley, C., Pfeifer, S., Preuschmann, S., Radermacher, C., Radtke, K., Rechid, D., Rounsevell, M., Samuelsson, P., Somot, S., Soussana, J.-F., Teichmann, C., Valentini, R., Vautard, R., Weber, B., and Yiou, P.: EURO-CORDEX: new high-resolution climate change projections for European impact research, Reg. Environ. Change, 14, 563–578, doi:10.1007/s10113-013-0499-2, 2014.

Jacob, D. J. and Winner, D. A.: Effect of climate change on air quality, Atmos. Environ., 43, 51–63, doi:10.1016/j.atmosenv.2008.09.051, 2009.

Jerrett, M., Burnett, R. T., Pope, C. A., Ito, K., Thurston, G., Krewski, D., Shi, Y., Calle, E., and Thun, M.: Long-term ozone exposure and mortality, New Engl. J. Med., 360, 1085–1095, doi:10.1056/NEJMoa0803894, 2009.

Jiménez-Guerrero, P., Montávez, J. P., Gómez-Navarro, J. J., Jerez, S., and Lorente-Plazas, R.: Impacts of climate change on ground level gas-phase pollutants and aerosols in the Iberian Peninsula for the late XXI century, Atmos. Environ., 55, 483–495, doi:10.1016/j.atmosenv.2012.02.048, 2012.

Juda-Rezler, K., Reizer, M., Huszar, P., Krüger, B. C., Zanis, P., Syrakov, D., Katragkou, E., Trapp, W., Melas, D., and Chervenkov, H.: Modelling the effects of climate change on air quality over Central and Eastern Europe: concept, evaluation and projections, Clim. Res., 53, 179–203, 2012.

Jury, M.: Evaluation of Global Climate Models as Regional Climate Model Drivers, Wegener Center for Climate and Global Change, University of Graz, 2012.

Katragkou, E., Zanis, P., Kioutsioukis, I., Tegoulias, I., Melas, D., Krüger, B. C., and Coppola, E.: Future climate change impacts on summer surface ozone from regional climate-air quality simulations over Europe, J. Geophys. Res.-Atmos., 116, D22307, doi:10.1029/2011JD015899, 2011.

Klimont, Z., Kupiainen, K., Heyes, C., Cofala, J., Rafaj, P., Höglund-Isaksson, L., Borken, J., Schöpp, W., Winiwarter, W., Purohit, P., Bertok, I., and Sander, R.: Global scenarios of air pollutants and methane: 1990–2050, in preparation, 2015.

Kotlarski, S., Keuler, K., Christensen, O. B., Colette, A., Déqué, M., Gobiet, A., Goergen, K., Jacob, D., Lüthi, D., van Meijgaard, E., Nikulin, G., Schär, C., Teichmann, C., Vautard, R., Warrach-Sagi, K., and Wulfmeyer, V.: Regional climate modeling on European scales: a joint standard evaluation of the EURO-CORDEX RCM ensemble, Geosci. Model Dev., 7, 1297–1333, doi:10.5194/gmd-7-1297-2014, 2014.

Langner, J., Engardt, M., and Andersson, C.: European summer surface ozone 1990–2100, Atmos. Chem. Phys., 12, 10097–10105, doi:10.5194/acp-12-10097-2012, 2012a.

Langner, J., Engardt, M., Baklanov, A., Christensen, J. H., Gauss, M., Geels, C., Hedegaard, G. B., Nuterman, R., Simpson, D., Soares, J., Sofiev, M., Wind, P., and Zakey, A.: A multi-model study of impacts of climate change on surface ozone in Europe, Atmos. Chem. Phys., 12, 10423–10440, doi:10.5194/acp-12-10423-2012, 2012b.

Lecœur, È. and Seigneur, C.: Dynamic evaluation of a multi-year model simulation of particulate matter concentrations over Europe, Atmos. Chem. Phys., 13, 4319–4337, doi:10.5194/acp-13-4319-2013, 2013.

Lecœur, È., Seigneur, C., Pagé, C., and Terray, L.: A statistical method to estimate $PM_{2.5}$ concentrations from meteorology and its application to the effect of climate change, J. Geophys. Res.-Atmos., 119, 3537–3585, doi:10.1002/2013JD021172, 2014.

Manders, A. M. M., van Meijgaard, E., Mues, A. C., Kranenburg, R., van Ulft, L. H., and Schaap, M.: The impact of differences in large-scale circulation output from climate models on the regional modeling of ozone and PM, Atmos. Chem. Phys., 12, 9441–9458, doi:10.5194/acp-12-9441-2012, 2012.

McGrath-Spangler, E. L., Molod, A., Ott, L. E., and Pawson, S.: Impact of planetary boundary layer turbulence on model climate and tracer transport, Atmos. Chem. Phys., 15, 7269–7286, doi:10.5194/acp-15-7269-2015, 2015.

Megaritis, A. G., Fountoukis, C., Charalampidis, P. E., Denier van der Gon, H. A. C., Pilinis, C., and Pandis, S. N.: Linking climate and air quality over Europe: effects of meteorology on $PM_{2.5}$ concentrations, Atmos. Chem. Phys., 14, 10283–10298, doi:10.5194/acp-14-10283-2014, 2014.

Meleux, F., Solmon, F., and Giorgi, F.: Increase in summer European ozone amounts due to climate change, Atmos. Environ., 41, 7577–7587, 2007.

Menut, L., Bessagnet, B., Khvorostyanov, D., Beekmann, M., Blond, N., Colette, A., Coll, I., Curci, G., Foret, G., Hodzic, A., Mailler, S., Meleux, F., Monge, J.-L., Pison, I., Siour, G., Turquety, S., Valari, M., Vautard, R., and Vivanco, M. G.: CHIMERE 2013: a model for regional

ACPD
15, 28361–28393, 2015

Uncertainty in climate impacts on air quality

V. E. P. Lemaire et al.

atmospheric composition modelling, Geosci. Model Dev., 6, 981–1028, doi:10.5194/gmd-6-981-2013, 2013.
Prybutok, V. R., Yi, J., and Mitchell, D.: Comparison of neural network models with ARIMA and regression models for prediction of Houston's daily maximum ozone concentrations, Eur. J. Oper. Res., 122, 31–40, doi:10.1016/S0377-2217(99)00069-7, 2000.
Schlink, U., Herbarth, O., Richter, M., Dorling, S., Nunnari, G., Cawley, G., and Pelikan, E.: Statistical models to assess the health effects and to forecast ground-level ozone, Environ. Modell. Softw., 21, 547–558, doi:10.1016/j.envsoft.2004.12.002, 2006.
Seinfeld, J. H. and Pandis, S. N.: Atmospheric Chemistry and Physics: From Air Pollution to Climate Change, John Wiley & Sons, Hoboken, New Jersey, 2008.
Skamarock, W. C., Klemp, J. B., Dudhia, J., Gill, D. O., Barker, D. M., Duda, M. G., Huang, X. Y., Wang, W., and Powers, J. G.: A Description of the Advanced Research WRF Version 3, NCAR, Boulder, Colorado, USA, 2008.
Slini, T., Kaprara, A., Karatzas, K., and Moussiopoulos, N.: PM_{10} forecasting for Thessaloniki, Greece, Environ. Modell. Softw., 21, 559–565, doi:10.1016/j.envsoft.2004.06.011, 2006.
Taylor, K. E., Stouffer, R. J., and Meehl, G. A.: An Overview of CMIP5 and the Experiment Design, B. Am. Meteorol. Soc., 93, 485–498, 2012.
Thunis, P., Pederzoli, A., and Pernigotti, D.: Performance criteria to evaluate air quality modeling applications, Atmos. Environ., 59, 476–482, doi:10.1016/j.atmosenv.2012.05.043, 2012.
van Vuuren, D., Edmonds, J., Kainuma, M., Riahi, K., Thomson, A., Hibbard, K., Hurtt, G., Kram, T., Krey, V., Lamarque, J.-F., Masui, T., Meinshausen, M., Nakicenovic, N., Smith, S., and Rose, S.: The representative concentration pathways: an overview, Climatic Change, 109, 5–31, doi:10.1007/s10584-011-0148-z, 2011.
Vano, J. and Lettenmaier, D.: A sensitivity-based approach to evaluating future changes in Colorado River discharge, Climatic Change, 122, 621–634, doi:10.1007/s10584-013-1023-x, 2014.
Varotsos, K. V., Giannakopoulos, C., and Tombrou, M.: Assessment of the impacts of climate change on European ozone levels, Water Air Soil Poll., 224, 1–13, 2013.
Vautard, R., Honoré, C., Beekmann, M., and Rouil, L.: Simulation of ozone during the August 2003 heat wave and emission control scenarios, Atmos. Environ., 39, 2957–2967, 2005.
Young, P. J., Archibald, A. T., Bowman, K. W., Lamarque, J.-F., Naik, V., Stevenson, D. S., Tilmes, S., Voulgarakis, A., Wild, O., Bergmann, D., Cameron-Smith, P., Cionni, I., Collins, W. J., Dalsøren, S. B., Doherty, R. M., Eyring, V., Faluvegi, G., Horowitz, L. W., Josse, B.,

Lee, Y. H., MacKenzie, I. A., Nagashima, T., Plummer, D. A., Righi, M., Rumbold, S. T., Skeie, R. B., Shindell, D. T., Strode, S. A., Sudo, K., Szopa, S., and Zeng, G.: Pre-industrial to end 21st century projections of tropospheric ozone from the Atmospheric Chemistry and Climate Model Intercomparison Project (ACCMIP), Atmos. Chem. Phys., 13, 2063–2090, doi:10.5194/acp-13-2063-2013, 2013.

ACPD
15, 28361–28393, 2015

Uncertainty in climate impacts on air quality

V. E. P. Lemaire et al.

ACPD
15, 28361–28393, 2015

Table 1. Statistical models per region that explain the average $PM_{2.5}$ concentrations during 1976–2005.

Regions	R^2	Meteorological variable 1	Meteorological variable 2
BI	0.199	PBL-height	Surface wind
IP	0.139	PBL-height	Specific humidity
FR	0.222	PBL-height	Near surface temperature
ME	0.494	PBL-height	Near surface temperature
SC	0.196	Specific humidity	Incoming short wave radiation
NI	0.347	PBL-height	Near surface temperature
MD	0.141	PBL-height	Surface wind
EA	0.516	PBL-height	Near surface temperature

Table 2. Statistical models per region that explain the daily maximum summer ozone levels during 1976–2005.

Regions	R^2	Meteorological variable 1	Meteorological variable 2
BI	0.225	Incoming short wave radiation	Specific humidity
IP	0.482	Near surface temperature	Incoming short wave radiation
FR	0.494	Near surface temperature	Incoming short wave radiation
ME	0.620	Near surface temperature	Incoming short wave radiation
SC	0.126	Near surface temperature	PBL-height
NI	0.560	Incoming short wave radiation	Near surface temperature
MD	0.311	Near surface temperature	Surface wind
EA	0.683	Near surface temperature	Specific humidity

ACPD
15, 28361–28393, 2015

Table 3. Predicted concentrations of summertime ozone and $PM_{2.5}$ per selected regions and per model. The ensemble mean and standard deviation are also calculated.

RCP8.5 2071–2100	Delta (future–historical)							
	Ozone max					$PM_{2.5}$		
GCM/RCM\Regions	EA	FR	IP	ME	NI	EA	ME	NI
CNRM-CM5-LR/RCA4	6.56	5.26	8.05	3.76	5.14	−0.76	−0.87	−0.94
CSIRO-Mk3-6-0/RCA4	12.47	10.82	10.55	8.85	9.61	−1.32	−1.90	−1.51
CanESM2/RCA4	17.22	12.06	11.88	11.23	11.27	−0.94	−1.39	−1.61
EC-EARTH/RACMO2	7.76	8.75	8.81	6.60	6.97	−1.19	−0.80	−1.10
EC-EARTH/RCA4	11.57	9.77	8.82	7.65	8.01	−0.82	−0.74	−1.06
GFDL-ESM2M/RCA4	8.40	5.71	8.25	4.33	6.25	−1.07	−1.07	−0.91
IPSL-CM5A-MR/RCA4	13.34	9.39	10.10	7.25	9.59	−0.99	−0.92	−1.42
IPSL-CM5A-MR/WRF	4.77	5.15	7.57	3.70	3.28	−1.05	−1.37	−1.07
MIROC5/RCA4	10.93	7.90	9.24	6.40	7.16	−0.97	−0.81	−1.21
MPI-ESM-LR/CCLM	7.79	7.33	9.59	4.33	7.34	−0.69	−0.49	−0.87
MPI-ESM-LR/RCA4	10.64	8.14	9.17	5.89	7.65	−0.94	−0.77	−1.19
NorESM1-M/RCA4	9.89	8.42	8.75	6.90	6.89	−0.77	−0.84	−1.08
Ensemble Mean	10.11	8.23	9.23	6.41	7.43	−0.96	−1.00	−1.16
Ensemble Standard Deviation	3.22	2.06	1.13	2.14	2.02	0.18	0.37	0.23

ACPD
15, 28361–28393, 2015

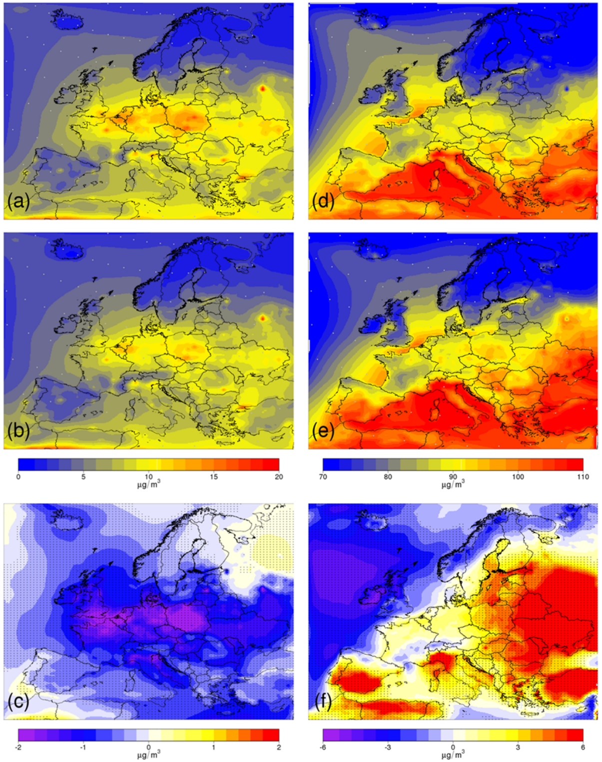

Figure 1. The left column represents daily average $PM_{2.5}$ concentrations for the historical (1976–2005) **(a)**, the end of the century (RCP8.5 – 2071–2100) **(b)** and the difference between the future and the historical **(c)**. The statistical significance of this difference is evaluated by a *t* test and represented by a black point. The right column presents the same figure for daily maximum ozone projections.

ACPD
15, 28361–28393, 2015
Uncertainty in climate impacts on air quality
V. E. P. Lemaire et al.

Title Page
Abstract | Introduction
Conclusions | References
Tables | Figures
◂◂ | ▸▸
◂ | ▸
Back | Close
Full Screen / Esc
Printer-friendly Version
Interactive Discussion

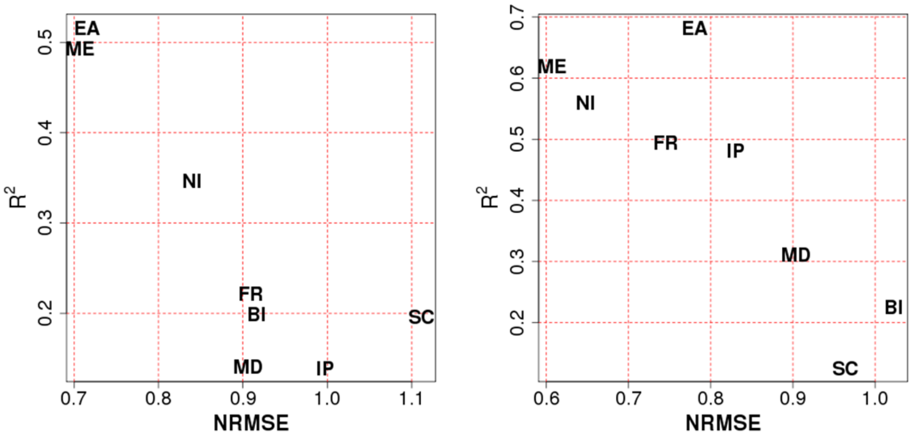

Figure 2. Linear model evaluation for $PM_{2.5}$ (left) and ozone (right). The x axis represents the Normalized Mean Square Error applied to the delta (future minus historical) of the linear model and chimere. The y axis represents the R^2 of the statistical model (training period).

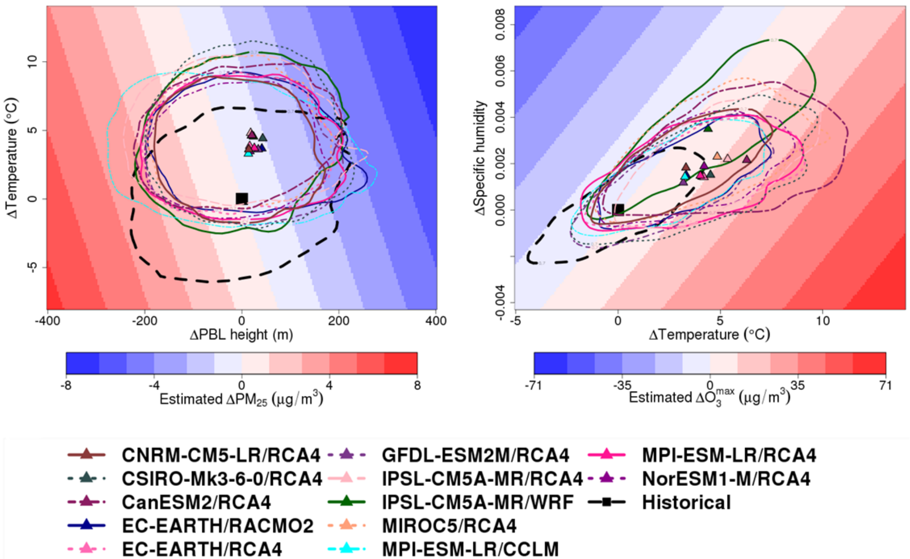

Figure 3. The left figure presents the proxy of ensemble projections for daily average de-seasonnalised $PM_{2.5}$ concentrations in Eastern Europe. The right figure represents the proxy for daily maximum de-seasonnalised summer ozone for Eastern Europe. For both figures, the shaded background represents the evolution of pollutants estimated by the statistical models. The contours are representing the regional climate projections and the triangles their mean. The black dashed contour represents the historical – IPSL-CM5A-MR/WRF – and the square its mean.

ACPD
15, 28361–28393, 2015

Uncertainty in climate impacts on air quality

V. E. P. Lemaire et al.

Title Page
Abstract | Introduction
Conclusions | References
Tables | Figures
◀ | ▶
Back | Close
Full Screen / Esc
Printer-friendly Version
Interactive Discussion

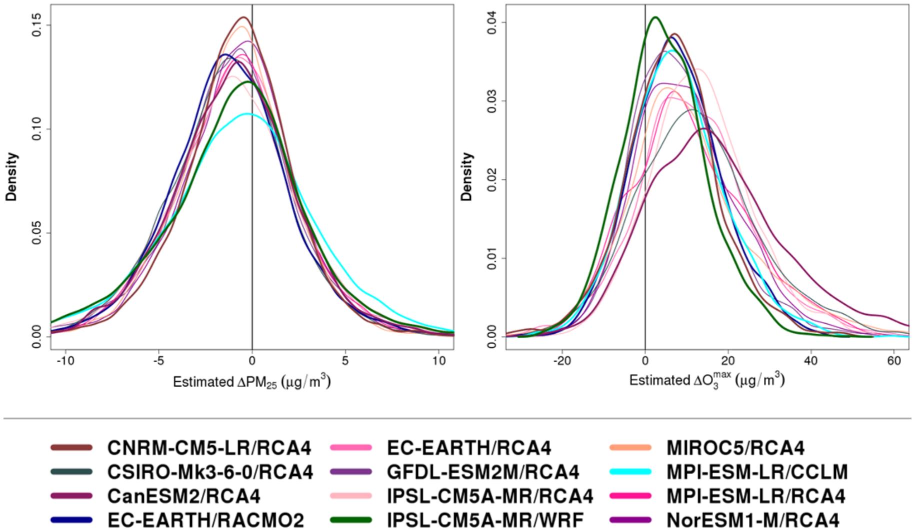

Figure 4. The left figure represents, for each regional climate model the probability density function (PDF) of the concentrations estimated with the bivariate linear model at the end of the century minus the estimated concentrations of the historical period for daily average de-seasonnalised $PM_{2.5}$ concentrations in Eastern Europe. The right figure presents the results for daily maximum de-seasonnalised summer ozone for Eastern Europe.

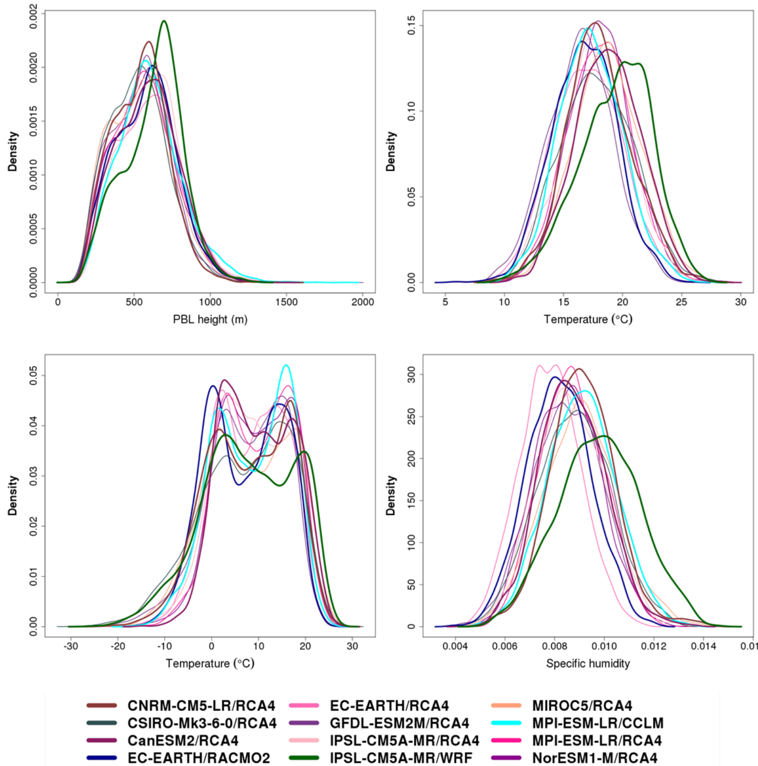

Figure 5. The first column of the panel represents the historical distribution of the meteorological variables identified by our statistical models as the two major drivers (**a** PBL Height; **b** near surface temperature) for $PM_{2.5}$ in Eastern Europe. The second column represents the historical JJA distribution of the two main drivers for summer ozone (**a** near surface temperature; **b** specific humidity).

ACPD
15, 28361–28393, 2015

Uncertainty in climate impacts on air quality

V. E. P. Lemaire et al.

Title Page
Abstract Introduction
Conclusions References
Tables Figures
◀◀ ▶▶
◀ ▶
Back Close
Full Screen / Esc
Printer-friendly Version
Interactive Discussion